

EVALUATION OF FRACTURE TOUGHNESS OF Zr-2.5 Nb PRESSURE TUBE MATERIAL AS A FUNCTION OF HYDROGEN CONTENT, DEFORMATION RATE AND TEMPERATURE

A. K. Bind, G. Sanyal, R. N. Singh, J. K. Chakravartty

Mechanical Metallurgy Division, Materials Group, Bhabha Atomic Research Centre, Mumbai-400-085

Email of corresponding author: akbind@barc.gov.in

ABSTRACT

In this investigation, J-R fracture characteristics of Zr-2.5Nb pressure tube material of Indian Pressurized Heavy Water Reactor (IPHWR) in cold worked and stress relieved condition have been evaluated over a range of loading rate, hydrogen content and at temperatures of 25 and 300°C. The fracture toughness tests have been carried out using 17 mm width curved compact tension specimens. Prior to testing these specimens have been gaseously hydrogen charged with hydrogen content up to 100 wppm. Both hydrogen charged and uncharged specimens have been tested at 25 and 300°C at five different pulling rates i.e. 0.02, 0.2, 2, 20 and 200 mm/min. The crack length during the fracture toughness tests has been measured using direct current potential drop technique. Various relevant fracture toughness parameters (J_Q , $J_{0.15}$, J_{Max} , $J_{1.5}$ and dJ/da) have been evaluated as per ASTM standard E1820.

It was observed that initiation fracture toughness for as received material did not change monotonically with loading rate at 25°C. The effect of loading rate on initiation toughness was most remarkable for as-received material at 300 °C as toughness increased with loading rate. However, for as received material tested at 300 °C, the crack propagation toughness parameters were not significantly influenced by loading rate. The effect of hydrogen content was very significant on fracture toughness parameters as the hydrogen content increased from 5 ppm for the as-received material to 60 ppm for hydrided material. With further increase in hydrogen content the toughness parameters were unaffected. For hydrided materials both crack initiation and propagation parameters were unaffected by increase in loading rate at 25°C. At 300°C for hydride materials, while initiation toughness exhibited a decreasing trend with increasing loading rate, propagation toughness values were apparently unaffected.

INTRODUCTION

Zr-2.5Nb alloy is used as pressure tubes in cold worked and stress-relieved (CWSR) condition in Indian Pressurized Heavy Water Reactor (IPHWR) and CANDU reactors [1-4]. Pressure tubes, also called coolant tubes, act as primary containment in these reactors, for hot heavy water coolant flowing at a pressure of around 10 MPa and at temperatures in the range of 250-300°C. Since it is a pressure boundary component, its integrity has to be demonstrated under reactor operating conditions [5-7]. An inherent problem with zirconium and its alloys is its affinity and low solid solubility for hydrogen. Though the specification limit for hydrogen content in the pressure tubes is 5 wppm for quadruple melted Zr-2.5Nb pressure tubes [8-9], part of the hydrogen/deuterium evolved during service from coolant-Zr-metal corrosion reaction is picked up by the pressure tubes [10-11] and at end of 30 years of designed life hydrogen content is expected to be less than 100 wppm under normal operating conditions. Hydrogen present in excess of terminal solid solubility (TSS) [12-13] precipitates out as hydride phase. Being brittle, the presence of substantial quantities of hydrides can cause embrittlement of the host matrix resulting in loss of ductility and impact and fracture toughness. However, for a significant reduction in these properties, certain minimum volume fraction of the embrittling phase [11] is required and the extent of embrittlement is strongly influenced by the orientation of hydride platelets.

The tubes for the Indian PHWRs [4] are manufactured following a fabrication route similar to but not exactly same as the modified route II developed for the pressure tubes of CANDU reactors [3,14]. The microstructure of CWSR Zr-2.5Nb pressure tube consists of heavily elongated and textured α -Zr grains surrounded by thin grain-boundary network of β -Zr phase [3-4]. Microstructural investigations suggest that the grain-size is finer and aspect ratio of α -Zr grains are smaller and circumferential basal pole texture is less pronounced for the Indian CWSR Zr-2.5Nb pressure tube material as compared to the CANDU pressure tube material.

A through defect assessment of a pressure boundary component such as pressure tube would require a reliable and large data base on the influence of hydrides on flow and fracture behavior. In addition to this, it must consider likely situations which impose low to intermediate to dynamic loading rates on the pressure tubes during normal and abnormal operating conditions. Further, Zr-2.5Nb pressure tube material is reported to exhibit dynamic strain ageing (DSA) which is known to affect flow and the fracture behavior [14]. In general a

material undergoing DSA, the loading rate has been found to influence both flow and fracture behavior significantly. Therefore a careful examination of the influence of hydrogen and rate of loading on flow and fracture properties is required to ensure that the results of structural integrity analysis are conservative. As regards hydride embrittlement which is one of the major life limiting factors for the pressure tube, several theoretical and experimental studies have been carried out to understand the influence of hydrogen/hydride on the mechanical properties in general and micro-mechanisms assisting crack nucleation and its propagation in the presence of hydride, in particular [9,15-24]. Chow et al. [22] reported fracture behaviour for pressure tube material obtained from CANDU reactors. However, no information is available in open literature on the influence of loading rate on the fracture behavior of as-received as well as hydrided CWSR Zr-2.5Nb alloy pressure tube used either in IPHWRs or in CANDU reactors. This paper describes our initial experimental study to understand the influence of rate of loading on hydrided and unhydrided material at 25°C and reactor operating temperature of 300°C.

EXPERIMENTAL

Material and Specimen

The material used in this study was from quadruple melted, autoclaved, unirradiated Zr-2.5Nb pressure tube of 235 MWe IPHWR. The chemical composition of quadruple melted Zr-2.5Nb pressure tube material is indicated in Table 1 [26]. The internal diameter of the tube was 81.5 mm with wall thickness of 3.7 mm. The typical values of room temperature yield and ultimate tensile strength of the material was 504 MPa and 733 MPa, respectively and the tensile elongation was 16 % in 25 mm gage length. The pressure tube sections of length 100 mm were polished up to 1200 grit emery paper to obtain oxide free surface and subsequently these tube sections were gaseously charged with target hydrogen concentration of 60 and 100 wppm in a modified Sievert's type apparatus [27]. The hydrogen charging was carried out at 363 °C and the charging duration at this temperature was about 1 h for maximum target hydrogen concentration of 100 wppm. The samples charged with lower amount hydrogen were also soaked for one hour at 363 °C so as to subject all the material to the same thermal cycle. Subsequently all the samples were homogenized for 24 h at 400°C to obtain uniform distribution of hydrides. Curved Compact Toughness (CCT) specimens of width 17 mm were machined out from these spools. The crack plane was along axial-radial plane to facilitate crack propagation along axial direction of the tube as described elsewhere [24].

Table 1: Typical chemical composition of Double melted Zr-2.5Nb alloy pressure tube material [26].

% Nb	Oxygen (ppm)	Carbon (ppm)	Fe (ppm)	Hydrogen (ppm)	Nitrogen (ppm)	Cl (ppm)	Cr (ppm)	Zr + permitted impurities
2.40 – 2.80	900 – 1300	125	<650	< 5	< 65	<0.5	<200	Balance

Fracture toughness testing

The CCT samples were fatigue pre-cracked to obtain sharp crack using sinusoidal cyclic loading at a frequency of 10 Hz. Fracture toughness tests were carried out as per ASTM E1820 method. The crack length was determined using direct current potential drop (DCPD) technique [16, 17, 24], which facilitated the use of single specimen technique for fracture toughness evaluation. The DCPD technique for estimating crack growth has been chosen over unloading compliance technique as it is particularly suitable at higher rates of loading. Due to curvature of the CCT specimens tapered pins were used to obtain uniform crack front across the thickness of the specimen. The stress intensity factor, K_I , for fatigue pre-cracking, calculated using *equation 1*, was reduced in four steps from the starting value of 15 to the final value of 10 MPa.m^{1/2} with the ratio of minimum to maximum load being maintained around 0.1.

$$K_I = \frac{P_Q}{BW^{1/2}} f(a/W) \quad (1)$$

where

$$f\left(\frac{a}{W}\right) = \frac{\left[2 + \frac{a}{W}\right] \left[0.886 + 4.64 \frac{a}{W} - 13.32 \left(\frac{a}{W}\right)^2 + 14.72 \left(\frac{a}{W}\right)^3 - 5.6 \left(\frac{a}{W}\right)^4\right]}{\left(1 - \frac{a}{W}\right)^{3/2}} \quad (2)$$

The value of a/W after fatigue pre-cracking was about 0.5. A servo-hydraulic UTM was used to pull the fatigue pre-cracked specimen in tension to facilitate mode I crack propagation on the axial-radial plane along axial direction of the tube. A resistance heated three-zone furnace fitted to the UTM was used for attaining high temperatures. The specimen was heated in air to the test temperature, soaked for an hour before starting the test. The specimens were pulled five at different rates i.e. 0.02, 0.2, 2, 20, and 200 mm/min. The temperature of the testing furnace was controlled during the test within 1°C through a K-type thermocouple, placed very close to the heating element, using a programmable temperature controller. The temperature of the CCT specimens was monitored using K-type thermocouple (0.2 mm dia.) spot welded to the inside curvature of the CCT specimens within 1 mm of the fatigue pre-crack tip. The crack growth was monitored using direct current potential drop technique [16, 17, and 24]. A constant DC current of 6 Amperes was used for all specimens. The DCPD output was measured during entire test duration using 0.2 mm diameter platinum wires spot-welded to the crack opening within 1 mm of the each side of the notch. The DCPD and thermocouple outputs were continuously recorded on a 12-channel video graphic recorder. Both fatigue crack length and the final crack length subsequent to fracture toughness testing were calculated from the nine equispaced readings along the crack front as per ASTM standard.

Computations

In this investigation the elastic and plastic component of J are calculated separately. The elastic component was computed from the load and using elastic constant of the material while the plastic component of J was calculated by normalizing the plastic area under the load (P) vs. load line displacement (LLD) curve. The procedure for computing J is given below [28]:

$$J_{(i)} = J_{e(i)} + J_{pl(i)} \quad (3)$$

where,

J_e = Elastic part of J-integral corresponding to i^{th} data point on load-displacement curve

J_{pl} = Plastic part of J-integral corresponding to i^{th} data point on load-displacement curve

The J_e is calculated as:

$$J_{e(i)} = \frac{K_{(i)}^2 (1 - \nu^2)}{E} \quad (4)$$

where,

$K_{(i)}$ = the value of K computed as equation (1) corresponding to i^{th} data point on load-displacement curve

$$\nu = \text{the poison ratio} = 0.436 - 4.8 \times 10^{-4}(T-300) \quad (5)$$

$$E = \text{the elastic constant} = 95900 - 57.4(T-273) \text{ MPa} \quad (6)$$

T = temperature in K

J_{pl} is calculated as:

$$J_{pl(i)} = \left[J_{pl(i-1)} + \frac{\eta_{(i-1)} (A_{pl(i)} - A_{pl(i-1)})}{b_{(i-1)} B} \right] \left[1 - \gamma_{(i-1)} \frac{(a_{(i)} - a_{(i-1)})}{b_{(i-1)}} \right] \quad (7)$$

where

$$\eta_{(i-1)} = 2.0 + \frac{0.522b_{(i-1)}}{W} \quad (8)$$

$$\gamma_{(i-1)} = 1.0 + \frac{0.76b_{(i-1)}}{W} \quad (9)$$

b = the remaining unbroken ligament

In equation (7) the quantity $[A_{pl(i)} - A_{pl(i-1)}]$ is the increment of plastic area under the force vs. plastic load line displacement record between lines of constant displacement at points $i-1$ and i shown in fig. 1 (shaded area). Thus

$$A_{pl(i)} - A_{pl(i-1)} = \frac{(P_{(i-1)} + P_{(i)}) (\delta_{(i)} - \delta_{(i-1)})}{2} \quad (10)$$

The various fracture toughness parameters were determined from the J-R curve generated for as-received as well as for hydrogen charged samples containing 60 and 100 wppm of hydrogen at 25 and 300 °C. For recording hydride morphology, the specimens were sectioned along radial-circumferential and radial-axial plane of the pressure tube. Standard metallographic technique was followed to reveal the hydride microstructure, its morphology and distribution. For optical microscopy the specimens were etched in a solution of HF:HNO₃:H₂O::2:9:9 for 15 seconds.

RESULTS

Microstructure

The current fabrication route of CWSR Zr-2.5 wt. % Nb pressure tubes produces a two phase microstructure of strongly textured and elongated (in axial direction) α -grains surrounded by very thin nearly continuous β -phase network along the grain-boundaries [29]. The α -grains, possess HCP structure, with basal poles predominantly aligned in the circumferential (transverse) or radial direction of the tubes. Figure 2 shows the three orthogonal directions of the pressure tube viz. Axial (A), Circumferential (C) and Radial (R) and AR – Axial-Radial, RC–Radial-Circumferential and AC–Axial-Circumferential planes schematically. Crystallographically permitted orientation of the hydride platelets in Zr-2.5Nb pressure tube alloy is also shown in this figure [11]. Typical α grain dimensions for the cold worked and stress-relieved Zr-2.5Nb pressure tube material is also indicated in this figure [29].

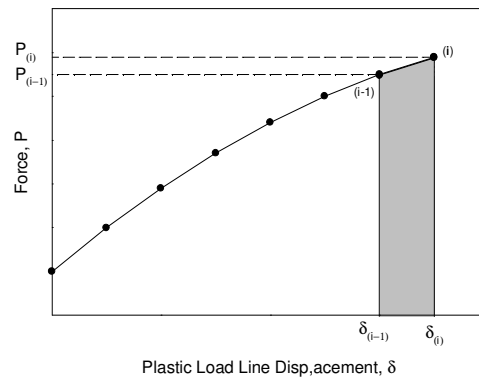


Fig.1. Definition of incremental plastic area under load-displacement for J plastic calculation

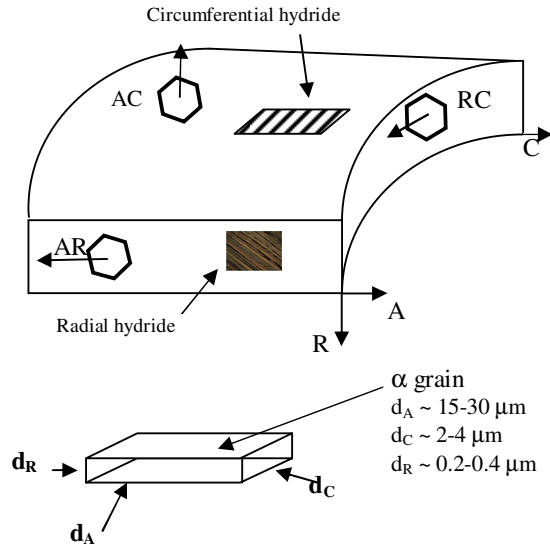


Fig. 2 A tube section illustrating the orientation of circumferential and radial hydrides[11] along with α phase grain dimensions²⁶ observed in CWSR Zr-2.5Nb pressure tube alloy.

The microstructural features of hydrides on RC plane of the Zr-2.5Nb pressure tube material, charged with (a) 60 and (b) 100 wt. ppm of hydrogen, are shown in fig. 3. This figure shows that in the as-hydrided condition, the traces of the hydride platelets (dark lines) are oriented along the circumferential direction only. These hydrides are called circumferential hydrides.

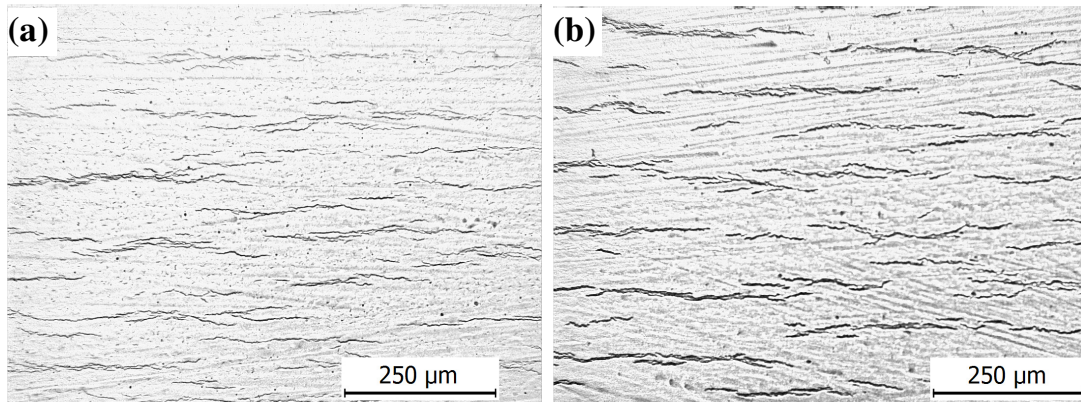


Fig. 3 The microstructure of Zr-2.5Nb pressure tube alloy charged with (a) 60 and (b) 100 wt. ppm of hydrogen revealing traces of hydrides (dark lines) on RC plane.

Influence of Loading Rate

Fig. 4 depicts a typical J vs crack extension (Δa) curve tested at 25°C. The blunting and exclusion lines are also shown in this figure to illustrate the computation of J_Q . The intersection of the 0.2 mm offset line and the best fit power law curve passing through the qualified J values were taken as J_Q . Apart from J_Q , the J values corresponding to intersection of construction lines passing through Δa of 0.15 mm and 1.5 mm with power law fit were also recorded. The value of J corresponding to maximum load value was also recorded. The slope of the best fit line passing through the qualified J values was taken as the mean dJ/da .

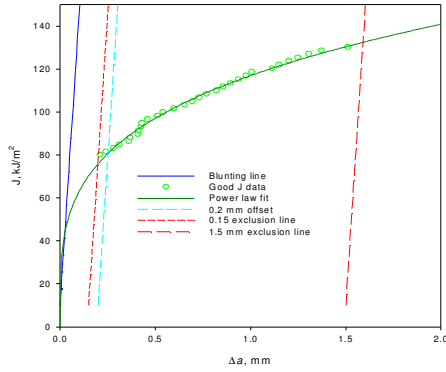


Fig. 4 A typical J vs Δa curve for the sample tested at 25 °C along with blunting and exclusion lines illustrates J_Q computation.

The fracture toughness parameters such as J_Q , $J_{0.15}$ and J_{Max} , $J_{1.5}$ and dJ/da were determined for each conditions of testing. For the sake of clarity, of the various fracture parameters we report only the variations of J_Q and dJ/da with loading rate, hydrogen content and temperature. Fig. 5 shows the influence of loading rate on (a) J_Q and (b) mean dJ/da values for Zr-2.5Nb pressure tube material at 25 and 300 °C. At 25 °C for the as-received material, the crack initiation parameter (J_Q) increased as the loading rate was increased from 0.02 mm/min to 0.2 mm/min (Fig. 5(a)). With further increase in loading rate the crack initiation parameters were observed to decrease with loading rate. At the same temperature, hydrided materials containing 60 and 100 ppm of hydrogen, exhibited much lower J_Q values and they were not significantly influenced by the loading rate. At 300 °C, for the as-received material the J_Q values increased as the loading rate increased from 0.02 to 200 mm/min. However for the sample charged with 60 wppm of hydrogen the initiation toughness first increased and then decreased with increase in loading rate. For the sample containing 100 wppm of hydrogen initiation toughness was observed to decrease with increase in loading rate.

The dependence of crack propagation parameter, dJ/da , on loading rate is shown in Fig. 5(b). At 25 °C for the as received material the propagation toughness parameter first increased to a maximum with increase in loading rate and then decreased with further increase in loading rate. At this temperature dJ/da values for hydride materials appeared to have a very weak dependency on loading rate. At 300 °C the dJ/da values were practically independent of loading rate for as-received as well as hydrided materials.

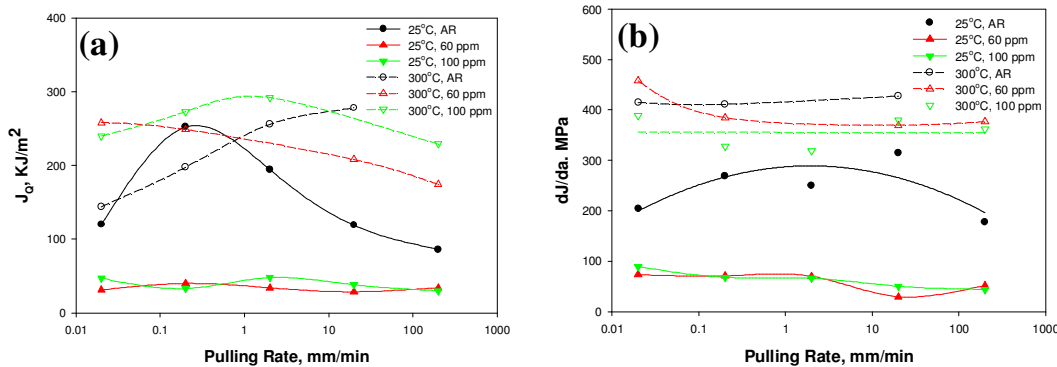


Fig.5. Influence of loading rate on (a) J_Q and (b) dJ/da values of Zr-2.5Nb pressure tube alloy at 25 and 300 °C.

Influence of hydrogen content

The dependence of fracture toughness parameters on hydrogen content is shown in Fig.6. At 25 °C and all loading rates, the crack initiation toughness reduced significantly as the hydrogen content increased from 5 to 60 wppm. With further increase in hydrogen content the initiation toughness remain unaffected. Interestingly the initiation toughness values obtained from the tests carried out at 300 °C were observed to increase with increase in hydrogen content for the tests carried at all loading rates. However, for the tests carried out at a loading rate of 200 mm/min the initiation toughness was much lower for the hydrided sample as compared to the as-received one. The propagation toughness parameters were observed to decrease with increase in hydrogen content both at 25 and 300 °C. Though the decrease in propagation toughness with increase in hydrogen content at 25 °C was more pronounced than that at 300°C, which probably is due to reduced volume fraction of hydrides at 300 °C as compared to that at 25 °C.

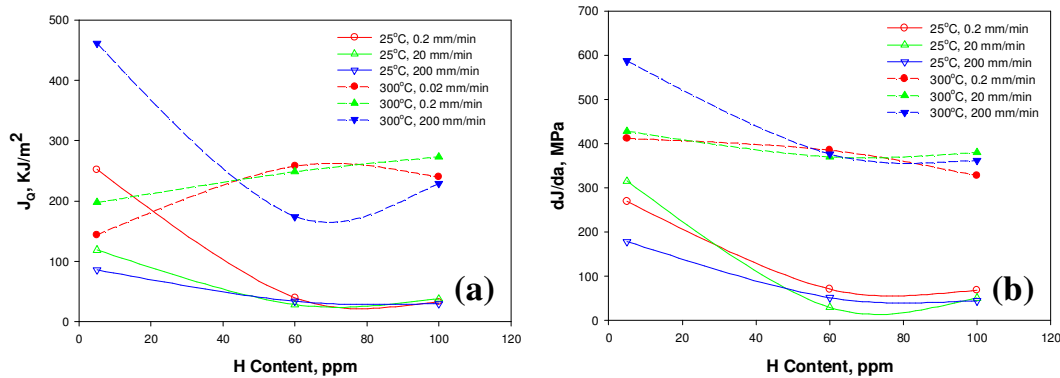


Fig. 6 Influence of hydrogen content on (a) J_0 , (b) $J_{1.5}$ and (c) dJ/da values of Zr-2.5Nb pressure tube alloy at 25 and 300 °C.

The study has shown that hydrogen has strong effect on both fracture initiation and propagation parameters which is a generally observed fact with CWSR Zr-2.5 Nb pressure tube material [21, 24]. Under quasi-static loading rates, it has been found earlier that initiation toughness parameters are not suitable for characterizing fracture behavior of pressure tube materials because of various reasons [24, 30, 31]. In contrast to this, propagation toughness parameter such as dJ/da has been found to be the most suitable and has been employed extensively in assessment of structural integrity [21, 31]. Thus the effects of loading rate on fracture toughness cannot be reliably ascertained using only initiation parameters. It may lead to misleading and non-conservative results. As regards the effect of loading rate on propagation toughness, it can be said that CWSR Zr-2.5Nb pressure tube exhibits good fracture resistance regardless of the loading rate at the reactor operating temperature and that propagation fracture toughness parameter is a weak function of loading rate. However additional tests at intermediate temperatures are needed to confirm the results reported here.

CONCLUSIONS

Fracture toughness parameters of cold worked and stress relieved Zr-2.5Nb pressure tube material were evaluated as a function of loading rate (0.02 to 200 mm/min) and hydrogen content (5-100 wppm). On the basis of the results obtained following conclusion can be drawn:

- Hydrogen has significant effect in lowering fracture toughness of Zr-2.5Nb pressure tube material
- Initiation toughness values did not monotonically change with loading rate for as received material. It is noted that there were no systematic trend for loading rate effect. For hydrided material, initiation toughness exhibited a lowering trend at 300°C and remained unaffected at 25°C with increasing loading rate.
- While propagation toughness values were found to increase with temperature and decrease with hydrogen content, the loading rate had no significant adverse effect on propagation toughness. In fact Zr-2.5Nb pressure tube exhibited a good fracture resistance at all loading rates of this investigation at both 25°C and reactor operating temperature.

References

- W. Dietz, "Structural Materials", in R. W. Cahn, P. Haasen & E. J. Kramer, (Eds.) *Materials Science & Techno. : A comprehensive treatment*, 10B Nuclear Materials, Chapter 8, (1994) 53.
- C. Lemaignan and A. T. Motta, "Zirconium alloys in nuclear applications", *ibid* 10B Chapter 7, (1994) 1.
- R. G. Fleck, E. G. Price, and B. A. Cheadle, "Pressure Tube Development for CANDU Reactors" *Zr in Nucl. Ind.*, D. G. Franklin and R. B. Adamson, Eds., ASTM STP 824, (1984) 88.
- R.N. Singh, P. Ståhle, J.K. Chakravarty, A.A. Shmakov (2009): "Threshold stress intensity factor for Delayed hydride cracking in Zr-2.5%Nb pressure tube alloy" *Mater. Sc. and Engg. A*, 523 (2009) 112.
- G. J. Field, J. T. Dunn, and B. A. Cheadle, "Analysis of the pressure tube failure at Pickering NGS "A" Unit 2 Nuclear Systems Department" *Can. Metall. Q.* **24(3)** (1985) 181.
- M. P. Puls, "Assessment of ageing of Zr-2.5Nb pressure tubes in CANDU™ reactors" *Nucl. Engg. & Design*, **171** (1997) 137.

7. G. D. Maon and P. J. Richinson "Leak before break in CANDU pressure tubes: Recent advances", *Pressure vessel and piping conference 1993*, Denver, CO, USA, 25-29 Jul 1993, (1993) 205.
8. J. R. Theaker, R. Choubey, G. D. Moan, S. A. Aldridge, L. Davis, R. A. Graham and C. E. Coleman, "Fabrication of Zr-2.5Nb pressure tubes to minimize the harmful effects of trace elements", *Zr in the Nucl Ind.: 10th Intl. Symp.*, Eds. E. R. Bradley and G. P. Sabol, *ASTM STP 1245* (1994) 221.
9. P. H. Davies, R. R. Hosbons, M. Griffiths and C. K. Chow, "Correlation between Irradiated and Unirradiated fracture Toughness of Zr-2.5Nb pressure tubes", *Zr in Nucl Ind.: 10th Intl. Symp.*, Eds A. M. Garde and E. R. Bradley, *ASTM STP 1245*, (1994) 135.
10. M. B. Elmoselhi, B. D. Warr and S. McIntyre, "A study of hydrogen uptake mechanism in zirconium alloys", *ibid.* (1994) 62.
11. D. O. Northwood, and U. Kosasih, "Hydrides and delayed hydrogen cracking in zirconium and its alloys," *Intl. Metals Rev.*, **28(2)** (1983) 92.
12. R. N. Singh, S. Mukherjee, Anuja Gupta and S. Banerjee, "Terminal solid solubility of hydrogen in Zr-alloy pressure tube materials" *Jl. of Alloys and Comp.*, 389 (2005) 102.
13. Z. L. Pan, I. G. Ritchie and M. P. Puls, "The terminal solid solubility of hydrogen and deuterium in Zr-2.5Nb alloys" *Jl. of Nucl. Mater.*, 228(2) (1996) 227.
14. R.N. Singh, S. Mukherjee, R. Kishore, B.P. Kashyap, "Flow behaviour of a modified Zr-2.5wt%Nb pressure tube alloy" *Jl. Nucl. Mater.* **345** (2005) 146.
15. R. N. Singh, R. Kishore, S. S. Singh, T. K. Sinha and B. P. Kashyap, "Stress-reorientation of hydrides and hydride embrittlement of Zr-2.5 wt% Nb pressure tube alloy" *Jl. Nucl. Mater.* **325** (2004) 26.
16. P. H. Davies and C. P. Sterns, "Fracture toughness testing of zircaloy -2 pressure tube material with radial hydrides using direct-current potential drop", in: J.H. Underwood, R. Chait, C.W. Smith, D.P. Wilhem, W.A. Andrews and J.C. Newman (Eds.) *ASTM STP 905*, (1986) 379.
17. F. H. Huang, "Fracture toughness evaluation for zircaloy-2 pressure tubes with the electric-potential method", *ASTM Intl. Symp. On Small specimen test techniques applied to nuclear reactor vessel thermal annealing and plant life extension*, New Orleans, LA, USA, 29-31 Jan 1992, (1993) 182.
18. K. S. Chan, "A fracture model for hydride-induced embrittlement", *Acta Metall. Mater.* **43(12)** (1995) 4325.
19. L. A. Simpson and C. K. Chow, "Effect of metallurgical variable and temperature on the fracture toughness of zirconium alloys pressure tubes", in *Zr in the Nucl. Ind.: 7th Intl. Symp.*, R. B. Adamson and L. F. P. Van Swam, (Eds.), *ASTM STP 939* (1987) 579.
20. S. I. Honda, "Fracture Toughness of Zr-2.5 wt% Nb Pressure Tubes" *Nucl. Engg. and Design*, **81** (1984) 159.
21. L. A. Simpson and C. D. Cann, "Fracture toughness of zirconium hydride and its influence on the crack resistance of zirconium alloys" *Jl. of Nucl. Mater.* **87** (1979) 303.
22. C. K. Chow, C. E. Coleman, R. R. Hosbons, P. H. Davies, M. Griffiths, and R. Choubey, "Fracture Toughness of Irradiated Zr-2.5Nb Pressure Tubes from CANDU Reactors" in *Zr in the Nucl. Ind.: 9th Intl. Symp.*, C.M. Eucken and A.M Garde, Eds. *ASTM STP 1132*, (1991) 246.
23. L. A. Simpson, "Criteria for fracture initiation at hydrides in zirconium-2.5 pct niobium alloy" *Metall. Trans.* **12A** (1981) 2113.
24. R. N. Singh, P. Stähle and N. S. Srinivasan, (2006) "Influence of Hydrogen Content on Axial Fracture Toughness Parameters of Zr-2.5Nb Pressure Tube Alloy in the Temperature Range of 306-573 K" Proc. of ICAPP '06 Reno, NV USA, June 4-8, 2006, Paper 6138.
25. J. W. Kim, I. S. Kim, "Investigation of dynamic strain ageing in SA106 Gr. C piping steel" *Nucle. Engg. Design* 171 (1997) 49-59.
26. K. Kapoor, K. Muralidharan, and N. Saratchandran, "Microstructure Evolution and Tensile Properties of Zr-2.5wt%Nb Pressure Tubes Processed from Billets with Different Microstructures" *Jl. of Mater, Engg. and Perform.* **8(1)** February (1999) 61.
27. R. N. Singh, R. Kishore, S. Mukherjee, S. Roychowdhury, D. Srivastava, B. Gopalan*, R. Kameswaran#, Smita S. Sheelvantra#, T. K. Sinha, P. K. De and S. Banerjee, "Hydrogen charging, hydrogen content analysis and metallographic examination of hydride in Zirconium alloys", BARC report No. BARC/2003/E/034, (2003) pp. 1-45.
28. ASTM Standard, E-1820-06.
29. D. Srivastava, G. K. Dey and S. Banerjee, *Metall. Trans. A*, **26A** 2707 (1995).
30. Candu Owner Group, Instructions to Round Robin Participants, COG-98-161-1, RC-2069, 1998, pp 21-28.
31. C. K. Chow, and L.A. Simpson., Fracture Mechanics: Eight Symposim, *ASTM STP 945*, 1988, pp. 419-439.